Enhancing Self-Cleaning Capabilities: Synthesis of Au Nanoparticle-Decorated MnO2 Thin Film with Photohydrophobic Behavior

Lanusubo Walling
Department of Electronics and communication engineering and Department of Science and Humanities
NIT, Nagaland
Dimapur, Nagaland
lanukun25@gmail.com

Stacy A. Lynrah
Department of Electronics and communication engineering
NIT, Nagaland
Dimapur, Nagaland
stacy038@gmail.com

P Chinnamuthu
Department of Electronics and communication engineering
NIT, Nagaland
Dimapur, Nagaland
chinnamuthu@nitnagaland.ac.in

J. P. Borah
Department of Science and Humanities
NIT, Nagaland
Dimapur, Nagaland
jpborah@nitnagaland.ac.in

Y Madhu Kumar
Department of Electronics and communication engineering
NIT, Nagaland
Dimapur, Nagaland
ymadhu522@gmail.com

PTSS Bhavana
Department of Electronics and communication engineering)
NIT, Nagaland
Dimapur, Nagaland
bhavanapurnaraju123@gmail.com

Palungbam Roji Chanu
Department of Electronics and communication engineering
NIT, Nagaland
Dimapur, Nagaland
rojichanu@gmail.com

***Abstract*— This study focuses on synthesizing MnO_2 thin films(TF) and Au-decorated MnO_2 TF using the E-beam evaporation technique to examine its wettability application. The X-ray diffraction (XRD) analysis demonstrates the preferred orientation and polycrystalline growth of the MnO_2 film. A contact angle goniometer was used to measure its contact angle, MnO_2 TF and MnO_2 TF/Au NP showed a contact angle of 112.2 and 104.2, respectively. Optical analysis revealed a significant UV and visible region enhancement for Au-decorated MnO_2 TF. Photoinduced hydrophilicity showed that MnO_2 TF/Au NP surpassed the bare MnO_2 TF. Introducing noble metal nanoparticles onto the MnO_2 TF contributed to this enhancement, which holds promise for various self-cleaning applications.**

Keywords*— MnO_2, nanoparticle, hydrophilicity, contact angle, and photocatalysis

I. Introduction

Photoinduced hydrophilicity behaviour of nanostructures primarily consisting of metal oxide has elicited considerable curiosity over the past few years due to its broad range of applications in the side view mirrors in self-cleaning glass, textiles, solar panels, and membranes. Photoinduced hydrophilicity refers to the property of a surface becoming more hydrophilic when exposed to light. This change occurs due to structural modifications at the surface caused by the diffusion of photogenerated holes[1]. Although the underlying mechanism is not fully comprehended, it has been observed in various thin films composed of metal oxides. The photoinduced hydrophilicity of films exhibited is attributed to the creation of hydroxyl groups, oxygen vacancies, and surface defects on the material surface. The conversion of the surface to a hydrophilic state upon irradiation is closely associated with photoinduced adsorption and photocatalysis[2]. Wetting models, such as the Wenzel and Cassie-Baxter models, have gained widespread usage in explaining the wetting behaviour of liquids on rough surfaces. The Wenzel model characterizes surfaces where droplets infiltrate the rough structures, leading to solid adhesive forces. Conversely, the Cassie-Baxter model describes rough surfaces where liquid droplets cannot penetrate but rest on top of the rough structures, resulting in weak adhesive forces[3][4]. Metal oxides with wide bandgaps, such as TiO_2, ZnO, and WO_3, have undergone extensive investigation for their potential applications as self-cleaning and antifogging surfaces [5], TiO_2 is one of the most extensively researched wide band gap metal oxides, has been widely investigated for its photoinduced hydrophilicity. With a wide band gap of 3.2 eV, TiO_2 exhibits remarkable photocatalytic properties, particularly in degrading organic pollutants. Its photoinduced hydrophilicity has garnered significant attention, as it holds promise for applications in self-cleaning glass, surface engineering, microfluidics, and biomedical devices. Another wide band gap, metal oxide, has attracted research attention. A particular study examined the photocatalytic activities of In_2O_3, SnO_2, and In_2O_3/SnO_2-doped titanium dioxide (ITO-TiO_2) samples [6]. The findings demonstrated that the addition of In_2O_3 and SnO_2 significantly enhanced the photocatalytic activity of ITO-TiO_2. Notably, the ITO-TiO_2 sample exhibited the highest photocatalytic activity among the tested samples. This indicates the potential of In_2O_3 in improving the photocatalytic performance of metal oxide-based systems. When exposed to UV irradiation, introducing gold nanoparticles to metal oxide systems can enhance their hydrophobic properties. This effect is attributed to the plasmonic characteristics of gold nanoparticles, which enhance UV light absorption and induce localized surface plasmon resonance (LSPR) effects. These LSPR effects lead to the generation of hot electrons that can transfer to the surface of the metal oxide, resulting in the reduction of

surface hydroxyl groups and the formation of a hydrophobic surface [2].

In a particular investigation, the impact of gold nanoparticles on the photoinduced hydrophobicity of TiO2 thin films was explored [7]. The findings demonstrated a significant enhancement in hydrophobicity when gold nanoparticles were incorporated into the TiO2 thin films and subjected to UV irradiation. The study also revealed that the degree of hydrophobicity depended on the size and concentration of the gold nanoparticles.

Similarly, another study examined the influence of gold nanoparticles on the photoinduced hydrophobicity of ZnO thin films. The results indicated a substantial increase in hydrophobicity when gold nanoparticles were added to the ZnO thin films and exposed to UV irradiation. The study further highlighted that the extent of hydrophobicity was influenced by the size and concentration of the gold nanoparticles [2].

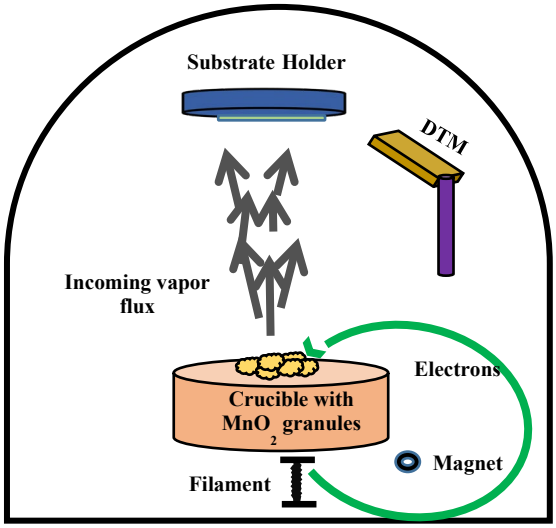

Fig. 1. Schematic diagram of E-beam evaporator machine

Electron Beam Evaporation (E-Beam Evaporation) is a widely used physical vapor deposition (PVD) technique that applies a dense, thin layer of coating onto substrates. This process takes place in a high-vacuum environment, employing a high-power electron beam to vaporize the coating material. As a thermal evaporation process, E-Beam Evaporation is a prominent PVD method alongside sputtering. Its key advantage lies in the direct transfer of substantial energy to the source material, enabling the evaporation of metals and dielectric substances with exceptionally high melting points, such as gold and silicon dioxide, respectively. E-Beam Evaporation serves the purpose of depositing materials that are challenging to evaporate through standard resistive thermal evaporation methods. The technique achieves higher deposition rates compared to sputtering or resistive evaporation, thanks to its superior heating capability, effective evaporation of high melting point materials (beneficial for refractory metals like tungsten and tantalum), high material utilization efficiency, and the production of films with higher density and enhanced substrate adhesion[28]. These advantages establish electron beam evaporation as a powerful and efficient method for rapid thin film deposition.

Manganese dioxide (MnO_2), a naturally occurring inorganic compound known as pyrolusite, finds diverse applications as a catalyst, in dry-cell batteries, as a pigment, in organic synthesis, and as a colorant in bodies and glazes. Several methods exist to synthesize thin films of MnO_2, such as self-assembly of MnO_2 nanoparticles, hydrothermal synthesis, and plasma-enhanced chemical vapor deposition [29].

The synthesis of MnO_2 thin films through E-beam evaporation involves several crucial steps. Initially, the substrate, commonly composed of materials like glass, silicon, or metal, undergoes meticulous cleaning to ensure a pristine surface. The process occurs within a high vacuum environment, facilitating unobstructed vapor flow from the MnO_2 source material and promoting the formation of a thin, high-purity coating [18]. Placed in a graphite crucible inside the vacuum chamber, the MnO_2 source material is subjected to intense and focused electron beams, rapidly heating and sublimating it. The resulting vaporized MnO_2 particles travel directly towards the substrate, leading to the deposition of a thin film. The technique's precision allows accurate control over the deposition time and evaporation rate, enabling precise thickness control of the resulting MnO_2 thin film [30].

Contact angle is the angle created at the point of contact between a liquid and a solid surface, precisely where the liquid-vapor boundary meets the solid [26]. It indicates how easily a liquid wet the solid surface and depends on the equilibrium between the attractive forces of the liquid and the solid and the cohesive forces within the liquid itself. By measuring the contact angle, one can gain insights into the surface characteristics of a material, including its texture, chemical makeup, and surface energy.

The Young's equation, also called the Young-Dupré equation, establishes a mathematical connection involving the contact angle, surface tension, interfacial tension at the liquid-solid interface, and the surface free energy of the solid material [27]. The equation is:

$$\cos\theta = (\gamma_{SV} - \gamma_{SL})/\gamma_{LV}$$

This expression describes the components involved in the contact angle (θ) phenomenon. It involves the solid-vapor surface tension (γ_{SV}), the solid-liquid interfacial tension (γ_{SL}), and the liquid-vapor surface tension (γ_{LV})[27].

Through this underlying study, the nature of the wettability of MnO_2 TF and Au-decorated MnO_2 TF have been thoroughly examined. The finding made in the paper is listed below:

- Water contact angle (WCA) of MnO_2 TF and MnO_2 TF/ Au NP were found to be 112.2° and 104° respectively.
- The photo induced-hydrophobicity of MnO_2 TF was observed to be from 112.2 to 90.72 and MnO_2 TF/Au NP to be from 104.2 to 80.85.

This transition of WCA of Au decorated MnO_2 TF from hydrophobic to hydrophilic surface opens many application avenues like self-cleaning, anti-icing and anti-fogging.

II. Experimental Details

Before any deposition, the substrate underwent a thorough cleaning process involving successive immersions in acetone, methanol, and deionized water for 5 minutes each. MnO_2 granules with a purity of 99.99% from Ultrananotech Pvt. Ltd was utilized for growing the desired thin film. In the E-beam machine, p-type Si was included, maintaining a pressure of 5 x 10^{-6}. MnO_2 TF was deposited at a rate of 1 Å/sec. The thickness of the MnO_2 TF was measured using a Digital Thickness Monitor (DTM). Gold nanoparticles with a size of 8 nm were subsequently grown on top of the as-deposited TF.

X-ray diffraction (XRD) analysis (utilizing Cu Ka radiation with a wavelength of 0.1540) was conducted for structural characterization. Water contact angle measurements were performed using a DMS-401 instrument from Kyowa Interface Science CO LTD, Japan. Optical characterization involved absorption analysis using a Hitachi F-7000 instrument. The samples were irradiated with a 298 nm wavelength UV lamp for 10 minutes, repeated for five cycles

III. Results and Discussions

E-beam evaporation offers several crucial advantages for synthesizing MnO2 thin films and Au NP/MnO2 TF. Firstly, it provides precise control over the deposited film's thickness, ensuring the coating material is applied with exactness to the desired thickness. Secondly, E-beam evaporation exhibits compatibility with a diverse range of substrates, including glass, silicon, and metal, enabling the deposition of the coating material on various substrate types. Lastly, the scalability of the E-beam evaporation process is a significant asset, allowing it to be applied to both small and large substrates, making it adaptable to different applications, whether for small-scale research or large-scale industrial production [31]. These combined advantages make E-beam evaporation a highly suitable and versatile technique for synthesizing MnO2 thin films and Au NP/MnO2 TF, offering precise control, broad substrate compatibility, and flexibility in production scale.

A. XRD analysis

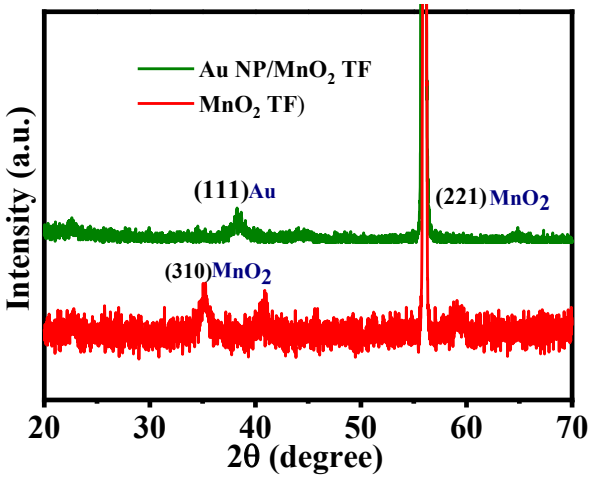

Fig. 2. XRD analysis of MnO2 TF and Au NP/MnO2 TF

Fig. 2 illustrates the structural analysis performed using X-ray Diffraction (XRD), which provides valuable insights into the crystallographic structure, chemical composition, particle size, defects, and other relevant information. The figure displays the XRD patterns of both MnO_2 Thin Film (TF) and Au NP/MnO_2 TF.

Regarding the as-deposited MnO_2 TF, the XRD pattern exhibits diffracted peaks at 56˚ and 35˚, corresponding to the (221) and (310) orientations of MnO_2, respectively. For the

Au NP/MnO2 TF, the XRD pattern reveals diffracted peaks at 38˚ (corresponding to Au) and 56˚ (corresponding to MnO2), with orientations of (111) and (221), respectively. These observations provide valuable information about the crystalline structures and orientations of the respective materials [24][25].

B. Absorption analysis

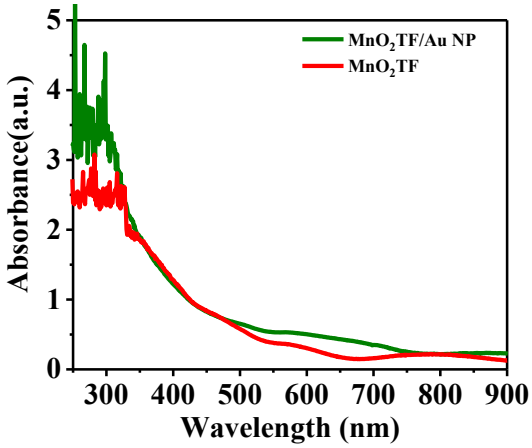

Fig. 3. Absorption analysis of MnO_2 TF and Au NP/MnO_2TF

Based on the findings in Fig. 3, the combination of Manganese dioxide (MnO2) and gold nanoparticles (Au NPs) results in a notable improvement in light absorption across both the UV and visible regions. This enhancement can be attributed to the Localized Surface Plasmon Resonance (LSPR) effect induced by the Au NPs, which leads to heightened light scattering and absorption.

C. Contact angle analysis

Table I presents the water contact angles (WCA) measured for the MnO_2 Thin Film (TF), Au-decorated MnO_2 TF samples. The water contact angle for MnO_2 TF is reported as 112.20. In contrast, for MnO_2 TF decorated with Au nanoparticles (Au NP), the contact angle is measured as 104.20. The introduction of Au NP onto the MnO_2 TF results in a decrease in the contact angle. This decrease can be attributed to increased surface energy, which reduces the contact angle[24][25].

TABLE I CONTACT ANGLE MEASUREMENTS OF MnO_2TF DECORATED WITH AU NP AND BARE MnO_2TF.

Sample	*Drop profile*	*Contact angle*
MnO_2 TF/Au NP		104°
MnO_2 TF	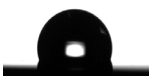	112.2°

D. Contact angle variation under UV illumination

The sample underwent UV radiation for 60 minutes, with 10 minutes of exposure each time. The decrease in

contact angle can be observed in Fig. 5. Compared to the bare MnO_2 TF. The Au-decorated MnO_2 TF exhibits a transition towards hydrophilicity, with the contact angles changing from 104.2° to 80.85° and 112.2° to 90.72°, respectively.

This change in contact angle can be attributed to the photocatalytic behavior of the MnO_2 TF. The presence of Au nanoparticles on the MnO_2 TF facilitates the trapping of photogenerated holes by oxygen atoms. As a result, the bonds with metal in the metal oxides are broken, and water molecules are adsorbed at these sites. This phenomenon is particularly prominent in oxides with easily created vacancies, such as TiO_2, ZnO, In_2O_3, and SnO_2[19].

Fig. 4. illustrates the behavior exhibited by MnO_2 Thin Film (TF) and MnO_2 TF decorated with Au nanoparticles (Au NP) upon exposure to UV light. When the MnO_2 TF absorbs UV photons, electrons from the valence band are excited to the conduction band, creating excess electrons in the conduction band. Simultaneously, holes occupy the valence band.

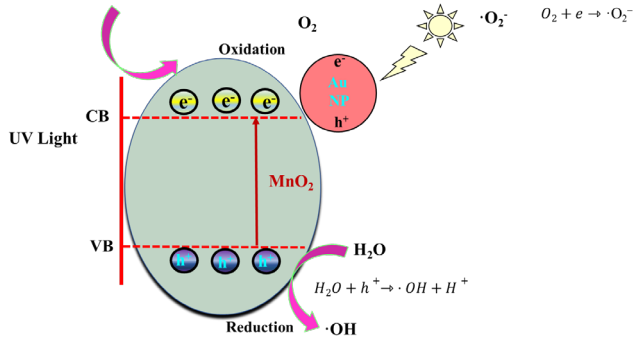

Fig 4. Photocatalytic behavior of MnO2 TF

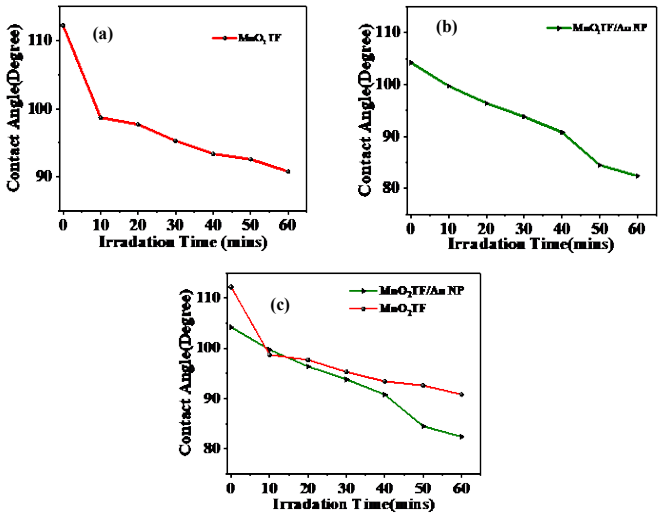

Fig. 5. Contact angle variation under UV illumination

It is important to emphasize that MnO_2 TF demonstrates remarkable oxidation and reduction capabilities, indicating its good reactivity. This exceptional reactivity arises from the ability of MnO_2 to undergo redox reactions, wherein it can either gain or donate electrons during chemical processes. This redox activity exhibited by MnO_2 TF makes it well-suited for diverse applications.

The presence of Au nanoparticles in the MnO2 TF further augments its photo response. This enhancement can be attributed to the plasmonic properties of Au nanoparticles, which enable efficient absorption of UV light, consequently inducing localized surface plasmon resonance (LSPR) effects. The LSPR effects facilitate electron transfer from the Au nanoparticles to the MnO2 TF, thereby influencing the redox behavior of MnO2 and potentially altering its reactivity.

Photocatalytic activity for removing pollutants. The possible reactions that occur in MnO_2 TF under UV irradiation are listed below:

$MnO_2 + hv \rightarrow e^- + h^+$

$MnO_2(h+) + H_2O \rightarrow \cdot OH + H^+$ (Hydroxyl radical)

$MnO_2(e-) + O_2 \rightarrow O_2^-$ (Superoxide anion radical)

Under UV illumination on MnO_2 TF, electrons transition from the valence band to the conduction band, accumulating excess electrons in the conduction band. These electrons can occupy the vacancies in the valence band. Consequently, the photoexcited electrons generate superoxide anion radicals (O2), while the holes interact with water molecules to produce hydroxyl radicals (OH*). This process leads to the degradation of pollutants.

The presence of Au nanoparticles on MnO_2 TF exhibits a pronounced UV-Vis absorption band. The decoration of Au nanoparticles on MnO_2 TF offers a promising approach for harnessing and utilizing UV light. This is evident from Fig. 3 and Fig. 5. (UV CA), where the Au-decorated surface demonstrates a faster transition and phase change from hydrophobic to hydrophilic. This behavior can be attributed to the higher rate of recombination between electron-hole pairs compared to the bare MnO_2 TF [19][20][21].

IV. Conclusion

Utilizing E-beam Evaporation technique MnO_2 thin film (TF) and Au-decorated MnO_2 TF were successfully synthesized. The water contact angle of Au NP/MnO_2 TF and pristine MnO_2 TF was found to be 104.2° and 112.2°, respectively. Remarkably under UV irradiation the Au NP/MnO_2 TF exhibits photo hydrophobicity as the WCA of it goes from 140.2° to 80.85°, thus a conversion from hydrophobic to hydrophilic nature of the surface presents a promising potential for self-cleaning applications.

Acknowledgment

The authors extend their gratitude to NIT Nagaland for granting access to essential research facilities. Special thanks are also given to the Physics Department, NIT Nagaland, for their assistance with XRD measurements

References

[1] .V. Rudakova & A.V.Emeline. (2021). Photoinduced Hydrophilicity of Surfaces of Thin Films. Colloid Journal. 83. 20-48. 10.1134/S1061933X21010105.

[2] M. Miyauchi, A. Nakajima, T. Watanabe, & K. Hashimoto. (2002). Photocatalysis and Photoinduced Hydrophilicity of Various Metal Oxide Thin Films. Chemistry of Materials - CHEM MATER. 14. 10.1021/cm020076p.

[3] A. Samanta,W. Qinghua. S.K. Shaw & H. Ding. (2020). Roles of chemistry modification for laser textured metal alloys to achieve extreme surface wetting behaviors. Materials & design. 192. 10.1016/j.matdes.2020.108744.

[4] A.B. Kamaraj, V. Shaw & M. Sundaram. (2015). Novel Fabrication of Un-Coated Super-Hydrophobic Aluminum via Pulsed Electrochemical Surface Modification. Procedia Manufacturing. 1. 10.1016/j.promfg.2015.09.081.

[5] L.C. Chen, C. M. Huang,C. S Gao & G. W. Wang. (2011). A comparative study of the effects of In2O3 and SnO2 modification on the photocatalytic activity and characteristics of TiO2. Chemical Engineering Journal. 175. 49–55. 10.1016/j.cej.2011.09.032.

[6] J. Y. Oh, B.R. Lee, H.M. Kim & C.H. Lee. (2015). Photoinduced Hydrophilicity of Heterogeneous TiO2/WO3 Double Layer Films. Journal of the Korean Institute of Electrical and Electronic Material Engineers. 28. 715-720. 10.4313/JKEM.2015.28.11.715.

[7] M. V. Maevskaya, A.V. Rudakova,A.V. Emeline & D.W Bahnemann, (2021)Effect of Cu2O Substrate on Photoinduced Hydrophilicity of TiO2 and ZnO Nanocoatings. Nanomaterial, 11, 1526. https://doi.org/10.3390/nano11061526

[8] X. Wang & Y. Li. (2003). "Synthesis and formation mechanism of manganese dioxide nanowires/nanorods." Chemistry–A European Journal 9,no.1, 300-306.

[9] J. W. Murray. (1975). "The interaction of metal ions at the manganese dioxide-solution interface." Geochimica et Cosmochimica Acta 39, no. 4 .505-519.

[10] B. Taranu, S. D. Novaconi, M. Ivanovici, J. N. Gonçalves, and S. F. Rus (2022). "α-MnO_2 Nanowire Structure Obtained at Low Temperature with Aspects in Environmental Remediation and Sustainable Energy Applications." Applied Sciences 12, no. 13 .6821.

[11] U. P. Shaik, S. Kshirsagar, M.G. Krishna, S. Tewari, D. D. Purkayastha & M. Vinjanampati. (2012). "Growth of superhydrophobic Zinc oxide nanowire thin films". Materials Letters. 75. 10.1016/j.matlet.2012.01.140.

[12] H. Chen, X. Li, and D. Li. (2022). "Superhydrophilic–superhydrophobic patterned surfaces: From simplified fabrication to emerging applications." Nanotechnology and Precision Engineering 5, no. 3 .035002,

[13] R. J. Isaifan, A. Samara, W. Suwaileh, D. Johnson, W. Yiming, A.A. Abdallah & B. Aïssa. (2019). Improved Self-cleaning Properties of an Efficient and Easy to Scale up TiO2 Thin Films Prepared by Adsorptive Self-Assembly." Materials science and technology 2, no. 3 .220-224.

[14] K. Reichelt and X. Jiang. (1990)."The preparation of thin films by physical vapour deposition methods." Thin Solid Films 191, no. 1 .91-126.

[15] C. Yang, H. Fan, Y. Xi, J. Chen, and Z. Li. (2008). "Effects of depositing temperatures on structure and optical properties of TiO_2 film deposited by ion beam assisted electron beam evaporation." Applied Surface Science 254, no. 9, 2685-2689.

[16] R. Zhang, G. M. Alushin, A. Brown, and E. Nogales. (2015)."Mechanistic origin of microtubule dynamic instability and its modulation by EB proteins." Cell 162, no. 4, 849-859.

[17] T. Ohmi. (1996). "Total room temperature wet cleaning for Si substrate surface." Journal of the Electrochemical Society 143, no. 9 .2957.

[18] P. Pooja, B. Choudhuri, V. Saranyan, and P. Chinnamuthu. (2019)."Synthesis of coaxial TiO_2/In_2O_3 nanowire assembly using glancing angle deposition for wettability application." Applied Nanoscience 9 .529-537.

[19] K. K. Kashyap, M. Hazarika, S. S. Dhayal, and P. Chinnamuthu. (2022)."Synthesis of metallic surface plasmon-sensitized TiO_2 nanowire for wettability application." Journal of Materials Science: Materials in Electronics 33, no. 11 .8674-8682,

[20] S. Xu, R. Sheng, Y. Cao, and J. Yan. (2017). "Reversibly switching water droplets wettability on hierarchical structured Cu_2S mesh for efficient oil/water separation." Scientific reports 9, no. 1.12486.

[21] R. Isaifan, A. Samara, W. Suwaileh, D. J. Johnson, W. Yiming, A. A. Abdallah, and B. Aïssa. (2017)."Improved self-cleaning properties of an efficient and easy to scale up TiO_2 thin films prepared by adsorptive self-assembly." Scientific reports 7, no. 1.9466.

[22] L. Duta, A. C. Popescu, I. Zgura, N. Preda, and 1. N. Mihailescu. (2015)."Wettability of nanostructured surfaces." Wetting and Wettability,no.7.pp.207-252.

[23] Y.Jia, S. Zhang, J. Zhang, L. Huang & F. Zhou. (2013). Effect of gold nanoparticles on the wettability of TiO_2 thin films. Applied Surface Science, 276, 765-769.

[24] S. A. Lynrah, and P. Chinnamuthu. (2022): "Spectral response of the MnO_2 thin-film photodetector based at room temperature." Materials Today: Proceedings 68 256-261.

[25] A. Riaz, A. Ashraf, H. Taimoor, S. Javed, M. A. Akram, M. Islam, M. Mujahid, I. Ahmad, and K. Saeed. (2019)."Photocatalytic and photostability behavior of Ag-and/or Al-Doped ZnO films in methylene blue and rhodamine B under UV-C irradiation." Coatings 9, no. 3 202.

[26] H.B.Eral, D.J.C.M.'t Mannetje & J.M. Oh, Contact angle hysteresis: a review of fundamentals and applications. Colloid Polym Sci 291, 247–260 (2013). https://doi.org/10.1007/s00396-012-2796-6

[27] Jun Yang,Yang Yang, Zhizhu He, Bowei Chen & Jing Liu (2015). A Personal Desktop Liquid-Metal Printer as a Pervasive Electronics Manufacturing Tool for Society in the Near Future. Engineering. 1. 506. 10.15302/J-ENG-2015042.

[28] N. ARSHI, J. LU, C.G. LEE, *et al.* Thickness effect on properties of titanium film deposited by d.c. magnetron sputtering and electron beam evaporation techniques. *Bull Mater Sci* **36**, 807–812 (2013).

[29] M M. Makhlouf (2018). Preparation and optical characterization of β-MnO2 nano thin films for application in heterojunction photodiodes. Sensors and Actuators A Physical. 279. 145 -156. 10.1016/j.sna.2018.06.003.

[30] Janky.Singh (2005). Review Nano and macro-structured component fabrication by electron beam-physical vapor deposition (EB-PVD). Journal of Materials Science.

[31] Hamid Fallah, Mohsen Ghasemi Varnamkhasti, Ali Hassanzadeh, & Hadi. Steki (2007). The effect of annealing on structural, electrical and optical properties of nanostructured ITO films prepared by e-beam evaporation. Materials Research Bulletin. 42. 487-496. 10.1016/j.materresbull.2006.06.024.